Efficient Polarization-Insensitive All-Fiber Wavelength Conversion in C-Band Using Feedback in Highly Non-Linear Fibers

Anadi Agnihotri, Arunabh Deka, and Pradeep Kumar Krishnamurthy

***Abstract*—We propose and experimentally demonstrate a novel dual-pump feedback-based polarization-insensitive wavelength conversion technique using four-wave mixing (FWM) in highly non-linear fiber (HNLF). By feeding the residual pumps at the output of the HNLF back to the fiber in orthogonal polarization state with respect to the original forward path pumps, we achieve approximately 6 dB improvement in FWM conversion efficiency with negligible polarization sensitivity. A simple theoretical treatment of polarization independent operation is presented. The experimental results closely match the theory and simulation results. Comprehensive comparisons with co-polarized dual pumps, orthogonal pumps, and single pump schemes highlight the significant reduction in polarization sensitivity from over 8 dB in the single pump scheme to approximately 0.7 dB, by the proposed scheme. As an application to the proposed technique, we experimentally demonstrate successful wavelength conversion of 10 and 20 Gbps 4-PAM format signals from 1552.58 nm to 1554.28 nm.**

***Index Terms*—Four wave mixing (FWM), optical wavelength conversion, fiber optic parametric amplifier (FOPA).**

I. Introduction

ALL-OPTICAL wavelength conversion (OWC) is a critical component in future high-capacity and long-haul wavelength division multiplexing (WDM) optical communication systems and are key in realizing all-optical networks [1], [2], [3]. It is essential for wavelength management, resolving spectrum conflicts, and optimizing optical networks to enhance blocking performance [4], [5]. Four-wave mixing (FWM) in optical fibers is widely used for OWC due to its instantaneous response of the fiber Kerr non-linearity which assures transparency to both bit-rate and modulation formats [6], [7]. However, conventional OWC schemes suffers from low conversion efficiency, limited bandwidth, and more importantly polarization sensitivity.

Manuscript received 2 February 2024; revised 2 May 2024; accepted 4 June 2024. Date of publication 7 June 2024; date of current version 28 June 2024. This work was supported by SERB, Department of Science and Technology India, under Grant SERB/CRG/2022/004079. *(Corresponding author: Anadi Agnihotri.)*

Anadi Agnihotri is with Photonics Science and Engineering, Indian Institute of Technology Kanpur, Kanpur 208016, India (e-mail: anadi.agnihotri@gmail.com).

Arunabh Deka is with Electrical Engineering, Indian Institute of Technology Kanpur, Kanpur 208016, India (e-mail: arunabh@iitk.ac.in).

Pradeep Kumar Krishnamurthy is with Electrical Engineering and Photonics Science and Engineering, Indian Institute of Technology Kanpur, Kanpur 208016, India (e-mail: pradeepk@iitk.ac.in).

Digital Object Identifier 10.1109/JPHOT.2024.3411039

Single pump based OWC schemes require precise control of the relative state of polarization (SoP) between the pump and signal inputs and suffers from limited bandwidth. This requirement poses a challenge in practical optical networks [8], [9]. The use of dual-pump FWM offers advantages over the single-pump scheme, addressing issues related to polarization sensitivity and spectral inversion [4]. It allows broadband wavelength conversion with the ability to maintain phase matching over a broader spectral range compared to single pump FWM. However, achieving simultaneous polarization insensitivity and wideband conversion in a dual-pump FWM wavelength converter is a challenge due to the opposing requirements for pump wavelength spacing - large for wideband operation and small for polarization-insensitive operation [6].

Various schemes have been employed to mitigate the polarization-dependence in all fiber OWC: a polarization diversity configuration for one-pump configuration [10], [11], the use of residual birefringence in a photonic crystal fiber (PCF) [12], and schemes involving two co-polarized pumps [4], [13], [14], or orthogonal-polarization dual-pumps [15], [16]. Orthogonal- and parallel-polarized dual-pump schemes involve using two pumps, each requiring precise SoP control. However, there are limitations on the wavelength detuning between the original signal and the pumps [4]. The polarization-diversity scheme, with a loop configuration in the nonlinear medium, limits conversion efficiency due to reduced contribution from orthogonal polarization pumps, and it may suffer from performance degradation due to backscattering and interference within the loop. Moreover, it includes 9.2 dB of passive losses in the whole subsystem [17], [18].

In this paper, we experimentally and theoretically demonstrate polarization insensitive all-optical wavelength conversion (PI-OWC) via feedback technique in a dispersion flattened HNLF. In this configuration, undepleted dual pumps are reintroduced into the highly nonlinear fiber (HNLF) via a polarization beam combiner (PBC). This scheme significantly enhances the conversion efficiency of the system by ≈ 6 dB. Additionally, it mitigates polarization-dependent loss, reducing it to a negligible 0.7 dB.

The rest of the paper is organized as follows. In Section II, we present the theoretical background of our proposed PI-OWC scheme. In Section III, we describe the experimental setup for PI-OWC and discuss the results of polarization insensitive, high conversion efficiency and broadband nature of our scheme. We apply our technique for wavelength conversion of 4-PAM signal

at 10 and 20 Gbps and discuss the results. Finally, in Section IV we conclude by summarizing our results.

II. Operation Principle

The basis of OWC is the non-degenerate FWM interaction in HNLF which exhibits third-order (Kerr) nonlinearity. The theory of FWM in silica optical fibers has been studied extensively [19], [20]. Before we discuss our proposed scheme for polarization-insensitive all-fiber OWC, we briefly review the conventional dual pump configuration for OWC. For details, please see [14], [15], [21]. Two co-polarized pump waves of frequencies ω_1 and ω_2 and a frequency spacing of $\Delta\omega$, co-propagating with a signal wave of frequency ω_3, interacts through Kerr nonlinearity in a dispersion flattened HNLF generating idler waves through FWM process. The pump and signal waves can be expressed as $\boldsymbol{E}_m(\omega_m,t)=\boldsymbol{A_m(z)}[\exp j(\omega_m t-k_m z+\varphi_m)]$, where $m=1,2$ represents pump 1 and 2 and $m=3$ represents signal lightwave. The FWM interaction is governed by wave equation, derived from Maxwell's equations and is given by

$$\left[\nabla^2+\frac{\omega_{id}^2}{c^2}\varepsilon\left(\omega_s\right)\right]\mathbf{E}_{id}\left(\omega_{id}\right)=-\mu_0\omega_{id}^2\mathbf{P}^{(3)}\left(\omega_{id}\right) \quad (1)$$

where $\boldsymbol{E}_{id}(\omega_{id},t)=\boldsymbol{A_{id}(z)}[\exp j(\omega_{id}t-k_{id}z+\varphi_{id})]$ is the electric field of the converted wave (idler), ε is the linear optical dielectric coefficient of the fiber, μ is the permeability and c is the velocity of light in a vacuum. The third-order electric polarization $\mathbf{P}^{(3)}$ term is given by

$$\begin{aligned}\mathbf{P}^{(3)}\left(\omega_{id}\right)=&\boldsymbol{\chi}^{(3)}\left(\omega'_{id}=\omega_1+\omega_2-\omega_3\right)\\&\vdots\mathbf{E}_1\left(\omega_1\right)\mathbf{E}_2\left(\omega_2\right)\mathbf{E}_3^*\left(\omega_3\right)\\&+\chi^{(3)}\left(\omega''_{id}=\omega_1-\omega_2+\omega_3\right)\\&\vdots\mathbf{E}_1\left(\omega_1\right)\mathbf{E}_2^*\left(\omega_2\right)\mathbf{E}_3\left(\omega_3\right)\\&+\boldsymbol{\chi}^{(3)}\left(\omega_{id}=-\omega_1+\omega_2+\omega_3\right)\\&\vdots\mathbf{E}_1^*\left(\omega_1\right)\mathbf{E}_2\left(\omega_2\right)\mathbf{E}_3\left(\omega_3\right)\end{aligned} \quad (2)$$

where $\boldsymbol{\chi}^{(3)}$ is third-order susceptibility tensor of the HNLF [22], [23].

Here we consider the converted light (idler) with frequency $\omega_{id}=\omega_3-\omega_1+\omega_2$ which corresponds to the third term in (2). Using the theory developed in [14], [15] which takes into account the random birefringence of fiber, the expression for $\mathbf{A}_{id}(z)$ can be obtained as

$$\mathbf{A}_{id}(z)=f_{s123}\lfloor\chi^{(3)}_{xxyy}\left(\mathbf{A}_1^*\bullet\mathbf{A}_3\right)\mathbf{A}_2+\chi^{(3)}_{xyyx}\left(\mathbf{A}_1\bullet\mathbf{A}_2^*\right)\mathbf{A}_3\rfloor \quad (3)$$

where

$$f_{s123}=\frac{j\mu_0\omega_s^2\sin(\Delta kz/2)}{k_s\Delta k}\exp j\left(\frac{\Delta kz}{2}\right) \quad (4)$$

is related to FWM conversion efficiency. Assuming phase matching, the electric field of the idler wave can then be expressed as

$$\begin{aligned}\boldsymbol{E}_{id}=&\left[r_{\omega_1,\omega_2}\left(\boldsymbol{A}_1\cdot\boldsymbol{A}_2^*\right)\boldsymbol{A}_3+r_{\omega_1,\omega_3}\left(\boldsymbol{A}_3\cdot\boldsymbol{A}_1^*\right)\boldsymbol{A}_2\right]\\&\cdot\exp j\left[\left(\omega_3-\omega_1+\omega_2\right)t+\left(\phi_3-\phi_1+\phi_2\right)\right]\end{aligned} \quad (5)$$

where r_{ω_i,ω_j} is the relative conversion efficiency coefficient due to the interaction grating generated by waves ω_i and ω_j [15]. The notation $\boldsymbol{A_i}\cdot\boldsymbol{A_j}$ indicates that the idler amplitude is dependent on the relative polarization angle of the electric fields $\boldsymbol{E}_i$ and $\boldsymbol{E}_j$. For short length fibers (200 m), the effect of polarization mode dispersion (PMD) is negligible as the diffusion length exceeds 1 km for $D_p<0.2\,ps/\sqrt{km}$ where D_p is the PMD parameter of the fiber. The relative orientation of the SoPs for all waves remains consistent along the fiber length [21].

Considering pump 1 and pump 2 to have polarization angle of θ and φ with respect to the signal, the power of the idler is approximately given by

$$P_1P_2P_3\left[r^2_{\omega_1,\omega_2}\cos^2(\theta-\varphi)+r^2_{\omega_1,\omega_3}\cos^2\theta\right] \quad (6)$$

where $P_i,\ i=1,2,3$ represents the power of the pumps and signal waves. The relative FWM conversion efficiency depends on the overlap integral of the pump and signal waves involved in the FWM interaction [see [14] for details]. We observe that the idler power is maximum for $\theta-\varphi=0$ which implies that pumps are co-polarized. However, the idler power is still sensitive to polarization due to the presence of second term which can be made zero by choosing $\theta=0$. This indicates that (6) is maximum when all three waves are co-polarized.

In order to obtain true polarization-insensitive operation, we propose the feedback-based dual pump PI-OWC. Fig. 1(a) shows the conceptual diagram of our proposed scheme. Two pumps (at $\omega_1$and ω_2) are launched into the HNLF via one port of the PBC. We assume that the pumps and signal waves are linearly polarized. The residual pumps after undergoing FWM in the HNLF, are filtered and then fed back into the HNLF via the second port of the PBC. The feedback loop includes a fixed optical delay and an optical amplifier to compensate for losses in the feedback path and filters. Subsequently, the signal to be wavelength converted, is combined after the PBC to eliminate any polarization-dependent loss due to coupling. The electric field at input of the HNLF is given by

$$\begin{aligned}\boldsymbol{E}_{in}=&\boldsymbol{E}_1\left(\omega_1,t\right)+\boldsymbol{E}_2\left(\omega_2,t\right)+\boldsymbol{E}_3\left(\omega_3,t\right)\\&+\left[\boldsymbol{E}_{1f}\left(\omega_1,t\right)a+\boldsymbol{E}_{2f}\left(\omega_2,t\right)\right]e^{j\delta}\end{aligned} \quad (7)$$

where $\boldsymbol{E}_{1f}$ and $\boldsymbol{E}_{2f}$ are the electric fields of the feedback pumps and δ is the phase delay obtained from delay line as shown in Fig. 1(a).

Using (6), an expression for various combination of polarization states of dual pumps (at fixed ω_1 and ω_2) in the feedback scheme, contributing to the idler power, can be derived. As shown in Fig. 1(b), θ_f and φ_f represents the SoP of signal with respect to feedback pumps - pump 1_f and pump 2_f. P_{1f} and P_{2f} corresponds to the power of feedback pumps. The idler power at $\omega_{id}=-\omega_1+\omega_2+\omega_3$ is given by:

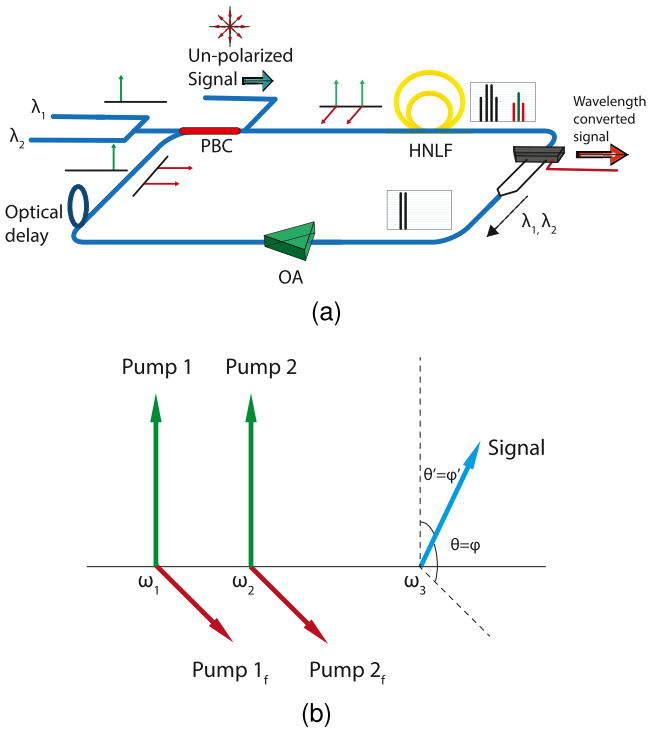

Fig. 1. (a) Schematic diagram of polarization insensitive feedback based wavelength conversion. (OA: Optical Amplifier, PC: Polarization Controller, PBC: Polarization Beam Combiner, HNLF: Highly Non-linear Fiber). (b) State of Polarization (SoP) of signal with respect to pumps.

- From interaction of co-polarized pumps 1 and 2 for which $\theta = \varphi$, we obtain the contribution to idler power

$$P_1 P_2 P_3 \left[r^2_{\omega_1,\omega_2} + r^2_{\omega_1,\omega_3} \cos^2\theta\right] \tag{8}$$

- From interaction of co-polarized pumps 1_f and 2_f for which $\theta_f = \varphi_f$, we obtain

$$P_{1f} P_{2f} P_3 \left[r^2_{\omega_1,\omega_2} + r^2_{\omega_1,\omega_3} \cos^2\theta_f\right] \tag{9}$$

- From interaction of orthogonally polarized pumps 1_f and 2 for which the first term in (6) vanishes and we get

$$P_{1f} P_2 P_3 \left[r^2_{\omega_1,\omega_3} \cos^2\theta_f\right] \tag{10}$$

- From interaction of orthogonally polarized pump 1 and 2_f for which the first term in (6) vanishes and we obtain

$$P_1 P_{2f} P_3 \left[r^2_{\omega_1,\omega_3} \cos^2\theta\right] \tag{11}$$

Since the feedback pump powers are made nearly equal to original pump powers by compensating for losses in the feedback path, we have $P_1 \approx P_{1f}$ and $P_2 \approx P_{2f}$ and using $\theta_f = 90^\circ - \theta$, from (8)–(11) the total idler power obtained from the feedback scheme is given by

$$P_{idf} = 2P_1 P_2 P_3 \left[r^2_{\omega_1,\omega_2} + r^2_{\omega_1,\omega_3}\right] \tag{12}$$

We see that the idler is invariant with respect to both polarization angles θ and φ as long as we satisfy the conditions leading to (8)–(11). Consequently, the conversion efficiency also improves, as can be seen from (12).

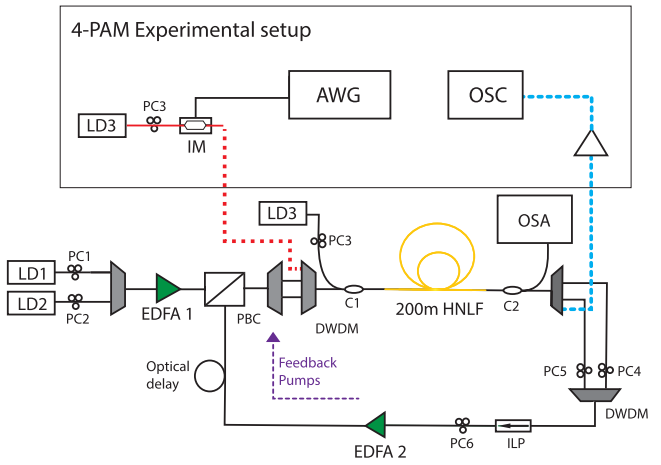

Fig. 2. Experimental setup of feedback scheme for PI-OWC. We also show the modification required for 4-PAM experiment. HNLF: highly non-linear fiber, DWDM: Dense wavelength division multiplexing Mux/DeMux, ILP: In-Line polarizer, PC: Polarization Controller.

III. Experimental Setup and Results

Fig. 2 shows the experimental setup of our proposed PI-OWC scheme. One of the dual-port tunable laser source (TLS, Keysight N7714 A), with an output power of -5 dBm and operating at a wavelength of 1549.32 nm, serves as pump 1, while a DFB laser source (Keysight 81663 A), with an output power of -5 dBm and a wavelength of 1550.92 nm, functions as the second pump (pump 2). The signal source is taken from the second output port of the TLS. The SoPs of all three–the two pumps and signal–can be set individually by adjusting the polarization controllers (PCs) as shown. The pump wavelengths are placed symmetrically around the zero-dispersion wavelength (ZDW) of the HNLF to ensure that the phase-matching condition is always satisfied [24].

The two pumps are combined using a DWDM Mux and amplified by EDFA (Optiwave AMP-901 A) after which they are fed to the first port of the PBC. A 4 channel DWDM Mux/Demux is used as optical filter to filter the ASE noise from the EDFA output. The pumps are then combined with signal wave using a 2×1 coupler and are coupled to a 200 m HNLF (OFS 80413Z0) for wavelength conversion. The input power of each pump into the HNLF is 10 dB. A 10% tap coupler is used to extract the optical signals from the HNLF output and measure the spectra on an OSA (Keysight 86142B). The output is attenuated by ≈ 8 dB before being measured by the OSA. The resolution bandwidth (RBW) of the OSA is set to 0.06 nm.

The HNLF used in our experiments has a nonlinear coefficient $\gamma = 10/\text{W-km}$, attenuation coefficient $\alpha = 0.5$ dB/km, ZDW = 1550 nm, and dispersion slope of 0.006 ps/nm^2 km. For the 200 m HNLF used in the experiment, fiber loss is negligible and we can consider any reduction in pump power to be due to FWM conversion. This is verified by our experiments by removing the feedback loop and measuring the optical spectrum at the HNLF output.

The undepleted pumps at the HNLF output are fed back to the HNLF input in a feedback loop as shown in Fig. 2. First,

the residual pumps - pump 1_f and pump 2_f are demultiplexed by a 16 channel DWDM Mux/Demux, their SoP is individually aligned using two PCs, and the SoP is set by an inline fiber polarizer (IFP) to ensure that the residual pumps are co-polarized. The feedback pumps are amplified using an EDFA to compensate for the losses in the feedback path. Subsequently, with adjustable optical delay, they are reintroduced to the HNLF via the second port of the PBC. The feedback pumps are orthogonally polarized with respect to the forward pumps coupled from the first port of the PBC. PC6 is used to tune the polarization of the pumps to ensure maximum coupling into the second port of the PBC.

A. *Optimization of Dual Pump Feedback Scheme*

Before considering OWC, we first optimize the experimental setup to obtain maximum FWM efficiency which depends on the phase mismatch and the relative polarization of the pumps [25], [26]. Since the phase mismatch is nearly zero due to placement of the pumps and dispersion flattened nature of our HNLF, we focus on the relative polarization of the pumps. This can be made sure by maximizing the power of the FWM products solely generated by the pump waves while disabling the signal source. When the FWM setup is maximized, the pumps are co-polarized with respect to each other and combine coherently in the PBC.

When the phase difference between the two input beams (pumps 1 and 1_f or pumps 2 and 2_f) is random, the polarization state of the combined beam is a superposition of polarization state of the two input beams [22], [27]. If the resultant polarization after PBC is circular for both the pumps then the four wave mixing efficiency decreases [20], [28]. Using an optical delay in the feedback path allows us to control the polarization of the resultant beam [29]. For an efficient system, the ellipticity of the combined beam is kept minimum by adjusting the optical delay.

The optical spectrum, recorded with and without feedback is shown in Fig. 3. The figure also shows the simulation results using Optisystem (version-17) commercial software. The simulation parameters have the same values as those of the components used in our experiment. The number of cavity iterations used for one simulation run is set to 10. To model the lightwave propagation in a nonlinear fiber, algorithm developed in [30] is used where first, the equations describing the signal propagation are solved by an iterative method (power analysis) and the power distribution along the fiber is calculated. Then, the signals are propagated using the vector nonlinear Schrödinger equation, which is solved using the split-step Fourier method to describe the dynamic interactions between the co-propagating signals.

The primary FWM components are generated at wavelengths 1547.88 nm and 1552.2 nm which agrees with theoretical values. We observe that the use of feedback improves the power of FWM components by approximately 7 dB. In the feedback setup, secondary FWM components are also generated as a result of interaction of pumps and the primary FWM components.

The signal is then turned on and coupled to the HNLF along with the pumps. The wavelength of the signal laser is varied across the C-band (1530–1560 nm) and the spectrum is recorded at the output of coupler C2. Fig. 5 shows the optical spectrum for the case of signal wavelength of 1555.87 nm. We observe

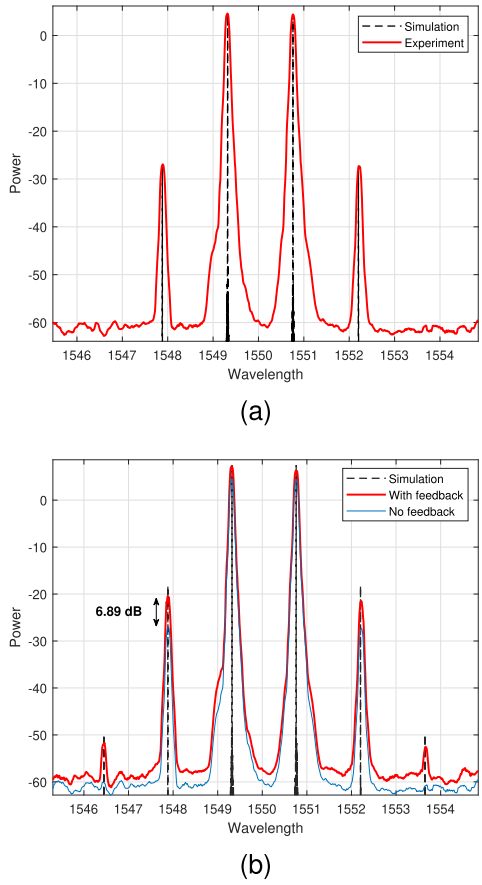

Fig. 3. (a) Spectrum without feedback (no signal input). (b) Spectrum with feedback (no signal input). The dash lines show the corresponding simulations. The 6.89 dB increase in primary FWM component in the feedback case ensures effective optimization of our PI-OWC scheme. The resolution bandwidth of the optical spectrum analyzer is set to 0.06 nm.

the idlers generated due to the interaction between signal and pumps at 1554.42 nm and 1557.35 nm.

B. *Comparison of Different Schemes*

The wavelength conversion efficiency (CE) is defined as a ratio of output idler to the input signal [31], [32], [33].

$$\eta = \frac{P_{idf}(\text{out})}{P_s(\text{in})} \tag{13}$$

where P_{idf} and P_s are idler and signal powers at output and input respectively. Fig. 4 shows the plot of conversion efficiency as a function of signal laser wavelength for different wavelength conversion schemes: single-pump in which pump P2 is turned off, orthogonal dual pumps, co-polarized dual pumps, and co-polarized dual pumps with feedback. The conversion efficiency is relatively low because of low input pump power and short length of HNLF (200 m). The total pump power in the HNLF is kept constant at 13 dBm throughout different schemes (single-pump, orthogonal and co-polarized dual pumps) which is also below the stimulated Brillouin scattering threshold of 16 dBm [34].

For the orthogonal pumps setup, feedback is turned off and the pumps (LD1 at 1549.32 nm and LD2 at 1550.90 nm) SoPs are orthogonally polarized through the polarization controllers

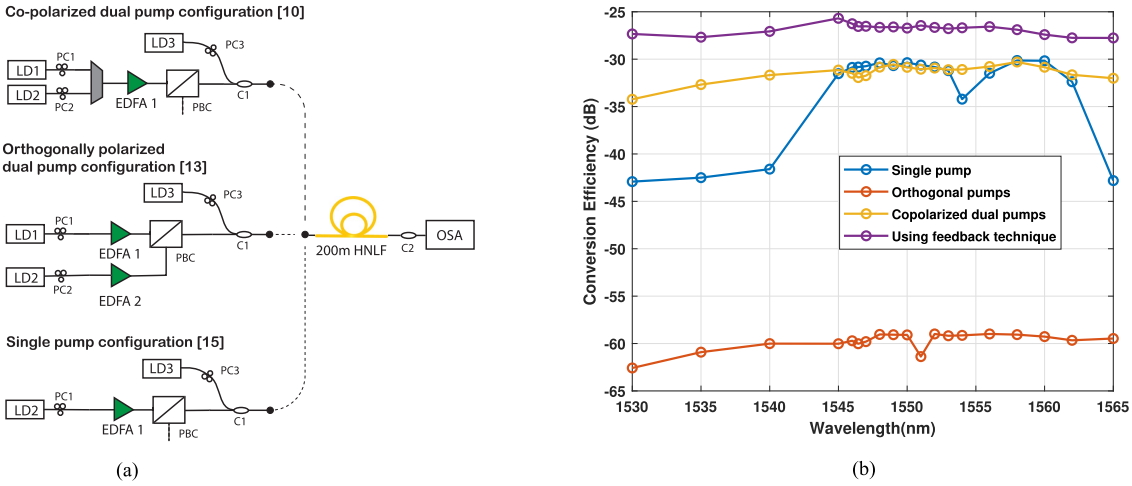

Fig. 4. (a) Experimental setups for FWM based wavelength conversion reported in the literature. (OA: Optical Amplifier, PC: Polarization Controller, PBC: Polarization Beam Combiner, HNLF: Highly Non-linear Fiber). (b) Conversion efficiency vs wavelength at different pump configurations. The experimental setups are similar to those employed in references indicated in [10], [13], and [15].

PC1 and PC2. This is made sure by using a polarization beam combiner to combine the two pumps. Pump powers at the input to HNLF is 10 dBm while the signal power remains at 0 dBm. The idler power is measured as a function of signal laser wavelength. The conversion efficiency remains very low as the signal wavelength is varied which agrees with previous results [14]. For comparison, we also show the result of co-polarized dual pump configuration without feedback in which the pump powers at the input to HNLF remains the same at 10 dBm and signal power at 0 dBm. For single-pump configuration, feedback is turned off and only LD2 (1552.90 nm) is used as the FWM pump. Optical power is increased to 13 dBm at the input to HNLF, for a fair comparison with the dual pumps, while the signal power remains at 0 dBm. The signal laser wavelength is tuned over the C-band and the idler power is measured as a function of signal laser wavelength. As can be seen from Fig. 4(b), the conversion efficiency exhibits large variations with respect to signal wavelength as expected [24]. The conversion efficiency as well as the bandwidth is significantly improved compared to orthogonal polarized dual pumps and single-pump configurations.

As seen from Fig. 4(b), the idler power variations with respect to signal wavelength for dual pumps with feedback (0.5 dB over C-band) remains less compared to the case without feedback. In addition, a higher conversion gain, by about 6 dB, is obtained by the use of feedback as can be seen from Fig. 4(b).

Fig. 6 shows the polarization sensitivity of the proposed scheme as the SoP of the signal laser is varied. The SoP of signal is varied by changing the QWP angle of the polarization controller PC3. We see that single-pump and co-polarized dual pumps configuration are highly sensitive to polarization changes in signal and exhibit approximately 8- and 5-dB variations over the QWP angle range. While the dual pump orthogonal polarized configuration performs when compared to the previous configurations, it still exhibits 6 dB variation as seen from Fig. 6.

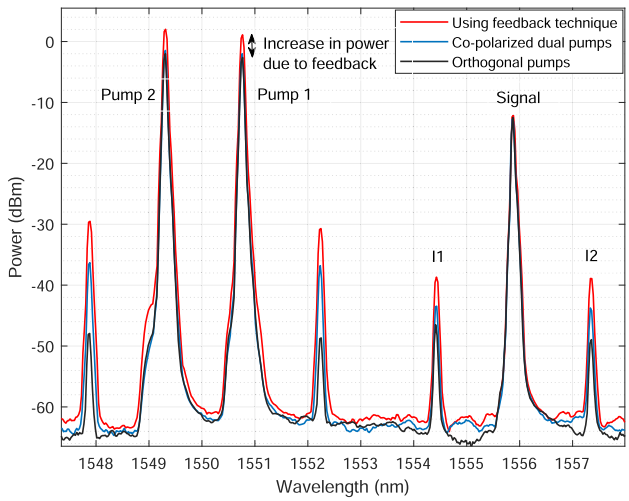

Fig. 5. Measured optical spectrum for signal at 1555.87 nm and pump 1 and 2 at 1549.32 nm and 1550.90 nm respectively at a resolution of 0.06 nm.

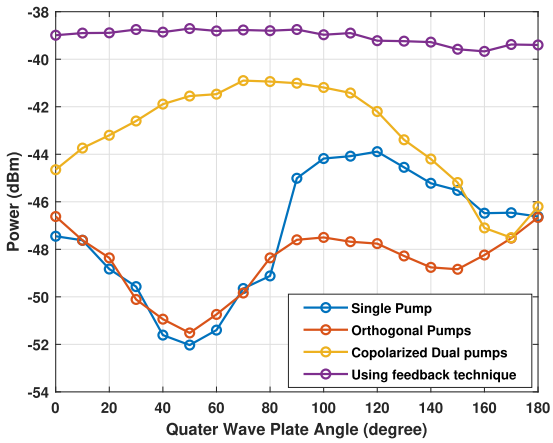

Fig. 6. Measured converted idler power as a function of quarter-wave plate angle of the PC.

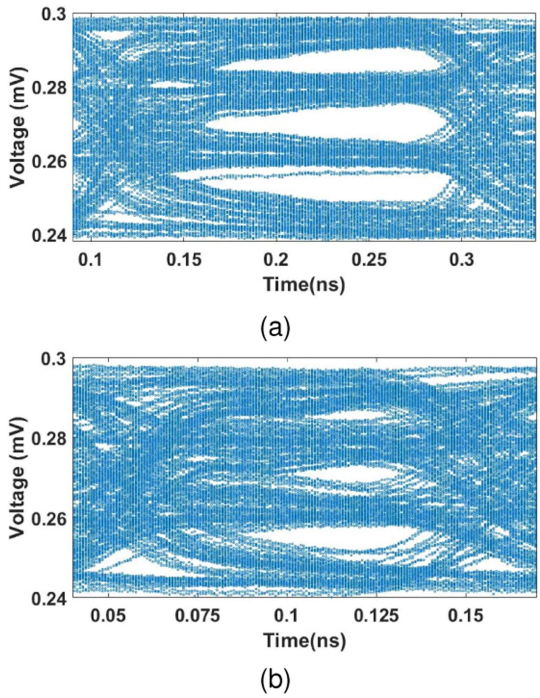

Fig. 7. 4-PAM eye diagram for (a) 10 Gbps (b) 20 Gbps, 2^9 PRBS sequence were used at both bit rates.

The use of feedback reduces the variations in idler power due to polarization changes to negligible 0.7 dB, thus exhibiting superior polarization insensitive operation. We attribute the 0.7 dB variation to a mismatch between optical power of pumps in forward and feedback path.

C. 4-PAM Results

We consider the performance of the proposed PI-OWC scheme for wavelength conversion employing 4 PAM transmission system. The experimental setup is shown in Fig. 2 where the signal laser (LD3) at wavelength 1552.58 nm is modulated by 4 PAM data and is then injected in the HNLF via DWDM Mux. The signal laser modulation is accomplished by a Mach-Zehnder modulator (MZM, Covega Mach-10) which is driven by a 2^9 PRBS sequence at 10 and 20 Gbps. The RF voltage pulses to the MZM is supplied by an arbitrary waveform generator (AWG Keysight M8195 A) which generated gaussian shaped voltage pulses of 1 Vpp. The PAM modulated optical signal is coupled to the PI-OWC scheme and detected at 1554.28 nm. The eye pattern recorded using Keysight sampling oscilloscope (DCA-X 86100D). From Fig. 7 we see that the eye is clear and open which remained in the same condition even when the SoP of the signal laser was varied using PC3. The eye is less clear at 20 Gbps bit rate. This is due to the insufficient amplitude from our RF devices and not due to the technique.

IV. Conclusion

In conclusion, we have proposed and experimentally demonstrated an efficient, polarization-insensitive all-fiber wavelength conversion method by employing feedback of residual pumps in a dual-pump four-wave mixing (FWM) configuration in a 200 m HNLF. We derived the expression for conversion efficiency and demonstrated polarization insensitivity across the C-band (1530–1565 nm) by adjusting the QWP angle. Furthermore, we have also experimentally demonstrated wavelength conversion based on this scheme for 10 Gbps and 20 Gbps PAM-4 signals. In direct comparison to existing methods, our approach offers a substantial increase in conversion efficiency of approximately 6 dB while maintaining negligible polarization sensitivity at 0.7 dB, outperforming orthogonal (5 dB), co-polarized (6 dB), and single pump (8 dB) schemes. It is to be noted that some wavelengths overlap with the pump and cannot be used. The performance of this scheme can be further optimized by implementing controlled feedback by monitoring the idler power then adjusting the feedback EDFA current and by using DPC (dynamic polarization controller) after the PBC. This scheme can also be used as an efficient fiber optic parametric amplifier (FOPA) at higher optical powers.

Acknowledgment

The authors would like to thank the reviewers for their constructive comments which helped improve the manuscript.

References

[1] L. Rau, W. Wang, S. Camatel, H. Poulsen, and D. Blumenthal, "All-optical 160-Gb/s phase reconstructing wavelength conversion using cross-phase modulation (XPM) in dispersion-shifted fiber," *IEEE Photon. Technol. Lett.*, vol. 16, no. 11, pp. 2520–2522, Nov. 2004.

[2] F. D. Ros, K. Dalgaard, L. Lei, J. Xu, and C. Peucheret, "QPSK-to-2BPSK wavelength and modulation format conversion through phase-sensitive four-wave mixing in a highly nonlinear optical fiber," *Opt. Exp.*, vol. 21, no. 23, pp. 28743–28750, Nov. 2013. [Online]. Available: https://opg.optica.org/oe/abstract.cfm?URI=oe-21-23-28743

[3] Y. Wu et al., "Generation of cascaded four-wave-mixing with graphene-coated microfiber," *Photon. Res.*, vol. 3, no. 2, pp. A64–A68, Apr. 2015. [Online]. Available: https://opg.optica.org/prj/abstract.cfm?URI=prj-3-2-A64

[4] C. Li et al., "Phase noise canceled polarization-insensitive all-optical wavelength conversion of 557-Gb/s PDM-OFDM signal using coherent dual-pump," *J. Lightw. Technol.*, vol. 33, no. 13, pp. 2848–2854, Jul. 2015.

[5] S. B. Yoo, "Wavelength conversion technologies for WDM network applications," *J. Lightw. Technol.*, vol. 14, no. 6, pp. 955–966, Jun. 1996.

[6] Y. Wang, C. Yu, T. Luo, L. Yan, Z. Pan, and A. E. Willner, "Tunable all-optical wavelength conversion and wavelength multicasting using orthogonally polarized fiber FWM," *J. Lightw. Technol.*, vol. 23, no. 10, pp. 3331–3338, Oct. 2005.

[7] Y. Gao, X. Chen, T. Cheng, F. Wang, and X. Yan, "Cascaded four-wave mixing all-optical wavelength converter based on highly nonlinear fiber deposited graphene oxide," *J. Mater. Sci. Technol.*, vol. 171, pp. 10–15, 2024.

[8] G.-W. Lu, T. Sakamoto, and T. Kawanishi, "Wavelength conversion of optical 64QAM through FWM in HNLF and its performance optimization by constellation monitoring," *Opt. Exp.*, vol. 22, no. 1, pp. 15–22, 2014.

[9] M. Matsuura, O. Raz, F. Gomez-Agis, N. Calabretta, and H. J. Dorren, "320 Gbit/s wavelength conversion using four-wave mixing in quantum-dot semiconductor optical amplifiers," *Opt. Lett.*, vol. 36, no. 15, pp. 2910–2912, 2011.

[10] H. Hu et al., "Polarization-insensitive all-optical wavelength conversion of 320 Gb/s RZ-DQPSK signals using a Ti: PPLN waveguide," *Appl. Phys. B*, vol. 101, pp. 875–882, 2010.

[11] K. Chow, C. Shu, C. Lin, and A. Bjarklev, "Polarization-insensitive widely tunable wavelength converter based on four-wave mixing in a dispersion-flattened nonlinear photonic crystal fiber," *IEEE Photon. Technol. Lett.*, vol. 17, no. 3, pp. 624–626, Mar. 2005.

[12] Y. Dai and C. Shu, "Widely tunable polarization-insensitive nondegenerate four-wave mixing wavelength conversion for DPSK signal," *IEEE Photon. Technol. Lett.*, vol. 22, no. 15, pp. 1138–1140, Aug. 2010.

[13] X. Li, J. Yu, Z. Dong, and N. Chi, "Wavelength conversion of 544-Gbit/s dual-carrier PDM-16QAM signal based on the co-polarized dual-pump scheme," *Opt. Exp.*, vol. 20, no. 19, pp. 21324–21330, Sep. 2012. [Online]. Available: https://opg.optica.org/oe/abstract.cfm?URI=oe-20-19-21324

[14] J. Ma et al., "Wavelength conversion based on four-wave mixing in high-nonlinear dispersion shifted fiber using a dual-pump configuration," *J. Lightw. Technol.*, vol. 24, no. 7, pp. 2851–2858, Jul. 2006.

[15] J. Lu, L. Chen, Z. Dong, Z. Cao, and S. Wen, "Polarization insensitive wavelength conversion based on orthogonal pump four-wave mixing for polarization multiplexing signal in high-nonlinear fiber," *J. Lightw. Technol.*, vol. 27, no. 24, pp. 5767–5774, Dec. 2009.

[16] M. A. Ettabib et al., "Polarization insensitive wavelength conversion in a low-birefringence Si-Ge waveguide," *IEEE Photon. Technol. Lett.*, vol. 28, no. 11, pp. 1221–1224, Jun. 2016.

[17] H. Hu et al., "Polarization-insensitive 320-Gb/s in-line all-optical wavelength conversion in a 320-km transmission span," *IEEE Photon. Technol. Lett.*, vol. 23, no. 10, pp. 627–629, May 2011.

[18] Y. W. Lee, K. J. Han, B. Lee, and J. Jung, "Polarization-independent all-fiber multiwavelength-switchable filter based on a polarization-diversity loop configuration," *Opt. Exp.*, vol. 11, no. 25, pp. 3359–3364, 2003.

[19] Y. Chen, "Four-wave mixing in optical fibers: Exact solution," *JOSA B*, vol. 6, no. 11, pp. 1986–1993, 1989.

[20] Q. Lin and G. P. Agrawal, "Vector theory of four-wave mixing: Polarization effects in fiber-optic parametric amplifiers," *JOSA B*, vol. 21, no. 6, pp. 1216–1224, 2004.

[21] G. P. Agrawal, "Nonlinear fiber optics," in *Proc. Nonlinear Sci. Dawn 21st Century*, 2000, pp. 195–211.

[22] P. Ma, R. Tao, X. Wang, Y. Ma, R. Su, and P. Zhou, "Coherent polarization beam combination of four mode-locked fiber MOPAs in picosecond regime," *Opt. Exp.*, vol. 22, no. 4, pp. 4123–4130, Feb. 2014. [Online]. Available: https://opg.optica.org/oe/abstract.cfm?URI=oe-22-4-4123

[23] K. Wang et al., "TiN/Ti3C2 heterojunction microfiber-enhanced four-wave mixing-based all-optical wavelength converter," *Photonics*, vol. 10, no. 10, 2023, Art. no. 1066.

[24] K. Inoue, "Four-wave mixing in an optical fiber in the zero-dispersion wavelength region," *J. Lightw. Technol.*, vol. 10, no. 11, pp. 1553–1561, Nov. 1992.

[25] K. Inoue and H. Toba, "Wavelength conversion experiment using fiber four-wave mixing," *IEEE Photon. Technol. Lett.*, vol. 4, no. 1, pp. 69–72, Jan. 1992.

[26] X. Jin, W. Bao, H. Zhang, Z. Zheng, and M. Zhang, "Four-wave mixing in graphdiyne-microfiber based on synchronized dual-wavelength pulses," *Photon. Res.*, vol. 10, no. 2, pp. 503–508, Feb. 2022. [Online]. Available: https://opg.optica.org/prj/abstract.cfm?URI=prj-10-2-503

[27] Y. Yang, C. Geng, F. Li, G. Huang, and X. Li, "Coherent polarization beam combining approach based on polarization controlling in fiber devices," *IEEE Photon. Technol. Lett.*, vol. 29, no. 12, pp. 945–948, Jun. 2017.

[28] D. N. Schimpf, T. Eidam, E. Seise, S. Hädrich, J. Limpert, and A. Tünnermann, "Circular versus linear polarization in laser-amplifiers with Kerr-nonlinearity," *Opt. Exp.*, vol. 17, no. 21, pp. 18774–18781, Oct. 2009. [Online]. Available: https://opg.optica.org/oe/abstract.cfm?URI=oe-17-21-18774

[29] Y. Yang, C. Geng, F. Li, and X. Li, "Combining module based on coherent polarization beam combining," *Appl. Opt.*, vol. 56, no. 7, pp. 2020–2028, Mar. 2017. [Online]. Available: https://opg.optica.org/ao/abstract.cfm?URI=ao-56-7-2020

[30] J. Ko, S. Kim, J. Lee, S. Won, Y. Kim, and J. Jeong, "Estimation of performance degradation of bidirectional WDM transmission systems due to Rayleigh backscattering and ASE noises using numerical and analytical models," *J. Lightw. Technol.*, vol. 21, no. 4, pp. 938–946, Apr. 2003.

[31] P. Apiratikul et al., "Enhanced continuous-wave four-wave mixing efficiency in nonlinear AlGaAs waveguides," *Opt. Exp.*, vol. 22, no. 22, pp. 26814–26824, Nov. 2014. [Online]. Available: https://opg.optica.org/oe/abstract.cfm?URI=oe-22-22-26814

[32] D. Yang et al., "Ultrahigh efficiency four-wave mixing wavelength conversion in packaged silica microrod resonator," *J. Lightw. Technol.*, vol. 41, no. 6, pp. 1768–1774, Mar. 2023.

[33] W. Mathlouthi, H. Rong, and M. Paniccia, "Characterization of efficient wavelength conversion by four-wave mixing in sub-micron silicon waveguides," *Opt. Exp.*, vol. 16, no. 21, pp. 16735–16745, Oct. 2008. [Online]. Available: https://opg.optica.org/oe/abstract.cfm?URI=oe-16-21-16735

[34] H. Hu et al., "640 Gbit/s and 1.28 Tbit/s polarisation insensitive all optical wavelength conversion," *Opt. Exp.*, vol. 18, no. 10, pp. 9961–9966, May 2010. [Online]. Available: https://opg.optica.org/oe/abstract.cfm?URI=oe-18-10-9961